

Design of Low-Complexity Convolutional Codes over GF(q)

Rami Klaimi, Charbel Abdel Nour, Catherine Douillard, Joumana Farah

▶ **To cite this version:**

Rami Klaimi, Charbel Abdel Nour, Catherine Douillard, Joumana Farah. Design of Low-Complexity Convolutional Codes over GF(q). GLOBECOM 2018 : IEEE Global Communications Conference, Dec 2018, Abu Dhabi, United Arab Emirates. 10.1109/GLOCOM.2018.8647824 . hal-01868752v2

HAL Id: hal-01868752

https://imt-atlantique.hal.science/hal-01868752v2

Submitted on 9 Nov 2018

HAL is a multi-disciplinary open access archive for the deposit and dissemination of scientific research documents, whether they are published or not. The documents may come from teaching and research institutions in France or abroad, or from public or private research centers.

L'archive ouverte pluridisciplinaire **HAL**, est destinée au dépôt et à la diffusion de documents scientifiques de niveau recherche, publiés ou non, émanant des établissements d'enseignement et de recherche français ou étrangers, des laboratoires publics ou privés.

Design of Low-Complexity Convolutional Codes over GF(q)

Rami Klaimi[1], Charbel Abdel Nour[1], Catherine Douillard[1], and Joumana Farah[2]

[1] IMT Atlantique, Lab-STICC, UBL, F-29238 Brest, France
[2] Department of Electricity and Electronics, Faculty of Engineering
Lebanese University, Roumieh, Lebanon

***Abstract*—This paper proposes a new family of recursive systematic convolutional codes, defined in the non-binary domain over different Galois fields GF(q) and intended to be used as component codes for the design of non-binary turbo codes. A general framework for the design of the best codes over different GF(q) is described. The designed codes offer better performance than the non-binary convolutional codes found in the literature. They also outperform their binary counterparts when combined with their corresponding QAM modulation or with lower order modulations.**

***Index Terms*—Finite field, non-binary codes, recursive systematic convolutional codes, coded modulation, turbo codes.**

I. Introduction

Since the early 2000s, binary turbo and low density parity-check (LDPC) codes [1], [2], [3], have been adopted in many communication standards, such as the third, fourth and fifth generations of mobile communications (3G, 4G, 5G), the second generation of digital video broadcasting (DVB) and the WiMAX standards. When transmitting long codewords, most of these codes are known to approach the Gaussian channel capacity very closely. However, they do not perform so close to the theoretical limit when small block lengths are considered [4]. The performance loss is due to the correlation experienced in the iterative decoding process of short data blocks [5].

These observations have triggered much attention from the channel coding research community, and are being taken into consideration with the increasing need for short packet transmission, for instance for machine to machine communications. In particular, numerous studies have investigated the design of codes over high-order Galois fields (GF), especially for the LDPC family, and have shown the potential of these codes [6], [7]. New structures of non-binary (NB) LDPC codes are proposed where the encoded NB symbols are directly mapped to a NB modulation with the same order. These codes are jointly designed with the corresponding modulation depending on the GF order.

While NB LDPC codes have been widely studied in the literature, research related to NB convolutional and turbo codes over GF(q), $q > 2$ is very limited. Convolutional codes over rings are defined in [8] using a matched mapping in order to easily find the best codes. In [9], [10], NB turbo codes are constructed derived from protograph sub-ensembles of regular LDPC codes. These codes are defined as a concatenation of two NB time-variant accumulators. Also, convolutional codes over GF(q) are defined in [11], where the author has limited the study to codes over GF(4). Using the results in [11], turbo codes over GF(4) are defined in [12]. In addition, turbo codes over GF(4) with different types of channels are studied in [13], [14]. A general study for the design of convolutional codes to be used as component codes for NB turbo codes over different GF(q) seems to be missing in the literature.

From an information theoretic perspective, previous studies have shown that bit-interleaved coded modulation (BICM) schemes suffer from a capacity loss compared to coded modulation (CM) schemes [15], [16]. This loss is even more pronounced for high modulation orders and at low spectral efficiencies. An example of comparison between the CM and BICM capacities is illustrated in Fig. 1, where a transmission with 64-QAM and QPSK modulations over an additive white Gaussian noise (AWGN) channel is considered. The BICM and CM capacities are calculated based on the model presented in [16].

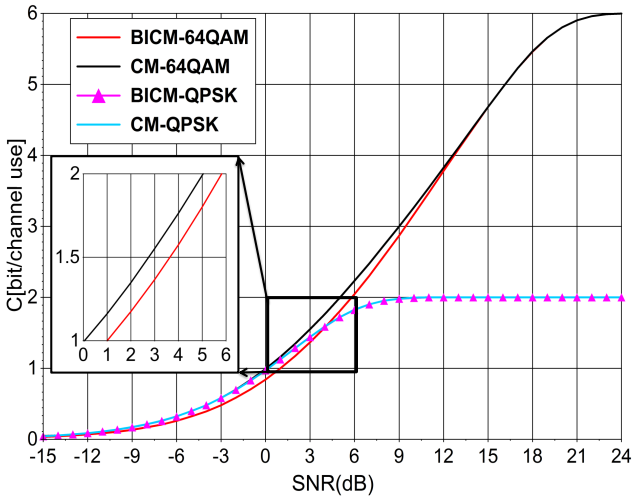


Fig. 1. BICM and CM capacities versus signal-to-noise ratio (SNR) over an AWGN channel.

Fig. 1 shows a gain in capacity of more than 1.0 dB for the coded modulation using 64-QAM for spectral efficiencies lower than 2 bit/channel use. In other words, a potential gain

of more than 1.0 dB of SNR can be achieved by using a NB coding scheme with coding rate 1/3 over GF(64) combined with a 64-QAM modulation, compared to a BICM scheme using binary coding. This is mainly due to the fact that, in the NB structure, the encoded symbols are directly mapped onto the modulation, instead of being marginalized as in the binary case. However, Fig. 1 shows almost equal CM and BICM capacities in the case of QPSK for all SNR regions. Therefore, from the capacity standpoint, there is no real interest in using codes over GF(4) combined with QPSK modulation.

From these results, one can assume that well-designed NB codes can outperform their binary counterparts for certain coding rate ranges and modulation orders. To this end, this paper presents a detailed study of the design of convolutional codes over NB GF(q), to be used as constituent codes for NB turbo codes.

This contribution is structured as follows: in section II we propose a new recursive systematic convolutional code structure over GF(q) and we show its superiority with respect to the classical structure with the same number of states. Section III starts by describing the used design criterion, then evaluates the impact of the constellation mapping on the search procedure. Simulation results comparing the proposed codes with the best published binary and non-binary convolutional codes in the state of the art are provided in section IV. Section V concludes the paper.

II. Non-binary recursive systematic convolutional code structures

In order to limit the complexity of the design process, only rate-$1/2$ convolutional codes with one memory element were considered in this work. First, the accumulator structure (structure S_1 in Fig. 2), inspired from the binary case, was used as an encoding template. Then, the proposed structure S_2 depicted in Fig. 2 was adopted for the reasons that will be presented shortly.

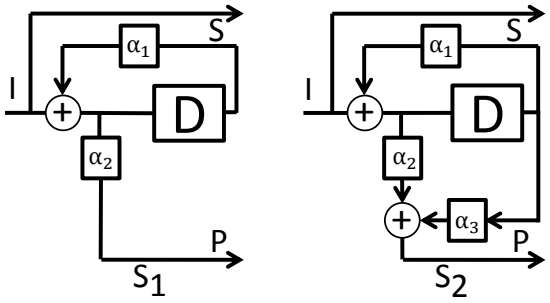


Fig. 2. Non-binary convolutional code structures with one memory element.

Both structures consist of a recursive systematic convolutional (RSC) code with recursion polynomial:

$$P_r(D) = 1 + \alpha_1 D \tag{1}$$

Note that the recursive nature of the code requires $\alpha_1 \neq 0$. The structures in Fig. 2 differ in the parity polynomial. For structure S_1, it is equal to:

$$P_{p_1}(D) = \alpha_2 + \alpha_2\alpha_1 D \tag{2}$$

and for structure S_2 to:

$$\begin{aligned} P_{p_2}(D) &= \alpha_2(1 + \alpha_1 D) + \alpha_3 D \\ &= \alpha_2 + (\alpha_1\alpha_2 + \alpha_3)\, D \end{aligned} \tag{3}$$

In order for structures S_1 and S_2 to represent a convolutional code, an additional constraint should be met in every structure. For structure S_1, it is sufficient to assume that $\alpha_2 \neq 0$. For S_2, we should have that:

$$\alpha_1\alpha_2 + \alpha_3 \neq 0 \tag{4}$$

When $\alpha_1\alpha_2 + \alpha_3 = 0$, the input data is just multiplied by a fixed coefficient without being encoded.

For a code defined over GF(q), coefficients α_j, $j = \{1, 2, 3\}$, the input data, systematic and parity output data are elements of GF(q). Since the encoding structures use only one memory element, the codes considered here have the lowest level of complexity, for a given value of q, among all the codes over GF(q). Their trellis diagrams have a number of states equal to the order of the Galois field and are fully connected.

Structure S_2 is more general than structure S_1 since the latter can be derived from the former by using the same coefficient α_1 and α_2 and by setting $\alpha_3 = 0$.

Let E_i and E_{i+1} be the encoder states at time i and $i+1$ and s_i and p_i be the systematic and parity symbols labeling the transition between E_i and E_{i+1}. The relation between the successive encoder states is, for both structures:

$$E_{i+1} = s_i + \alpha_1 E_i \tag{5}$$

For structure S_1, the parity symbol labeling the transition between E_i and E_{i+1} can be written as:

$$p_{1,i} = \alpha_2 \left(s_i + \alpha_1 E_i\right) = \alpha_2 E_{i+1} \tag{6}$$

For structure S_2, it is written as:

$$p_{2,i} = \alpha_2 \left(s_i + \alpha_1 E_i\right) + \alpha_3 E_i = \alpha_2 E_{i+1} + \alpha_3 E_i \tag{7}$$

If we assume that coefficients α_j, α_2 and α_3 are non-zero, $(q-1)^2$ different NB convolutional codes can be obtained with structure S_1 when varying the coefficients, while structure S_2 can provide $(q-1)^3$ different codes. For both structures, (5) shows that for a given value of α_1, q transitions stem from each state E_i, ending in q different possible states E_{i+1}. Equation (5) also shows that these q transitions are labeled with q different values of systematic symbols. Equations (6) or (7) provide the corresponding q different values of parity symbols for the two structures considered in this paper. The main difference between structures S_1 and S_2 is that the parity symbol $p_{1,i}$ is the same for the q transitions arriving at state E_{i+1} in S_1 due to (6). On the contrary, (7) shows that a non-zero value of α_3 allows all the transitions arriving at state

E_{i+1} in S_2 to be labeled with q different parity values $p_{2,i}$. Consequently, structure S_2 allows the search space for the code to span all the combinations of systematic and parity symbols for each transition between two states in the trellis.

III. Searching for good NB convolutional codes

A. Design Criterion

Going back to Ungerboeck's results on trellis codes [17], the selection criterion for a code, when associated with a high-order modulation, is based on the Euclidean distance spectrum of the coded modulation instead of the Hamming distance spectrum of the code, when no bit interleaving is considered. As far as NB convolutional codes are concerned, their selection is usually based on the minimization of the average symbol error probability P_s, which is upper bounded by [18]:

$$P_s \leq \sum_{I \in \mathcal{S}} \sum_{\hat{I} \in \mathcal{S}} n(I, \hat{I}) p(I) P(I \rightarrow \hat{I}) \tag{8}$$

where $\mathcal{S}$ denotes the set of different possible sequences in the trellis, I and $\hat{I}$ are the information sequences corresponding respectively to the correct path and to an erroneous path in the trellis, $p(I)$ is the probability that the source transmits sequence I, $P(I \rightarrow \hat{I})$ is the pairwise error probability (PEP), that is, the probability that the decoder chooses erroneous sequence $\hat{I}$ instead of the correct transmitted sequence I, and $n(I, \hat{I})$ is the number of erroneous symbols due to such an error event. For the case of an AWGN channel, deriving the Chernoff bound for the PEP [19], [20] gives:

$$P(I \rightarrow \hat{I}) \leq e^{-\frac{E_s}{4N_0} \sum_{n=1}^{N} |I_n - \hat{I}_n|^2} \tag{9}$$

where E_s is the average energy per transmitted symbol for the considered constellation $\mathcal{C}$. Therefore, minimizing the average symbol error probability amounts to maximizing the Euclidean distance between sequences in the trellis diagram, which is our primary objective in this study.

Contrary to binary convolutional codes, when associated with a high order modulation, the first terms of the distance spectrum of a NB code cannot be obtained by assuming that the all-zero sequence has been transmitted. This is due to the fact that common NB constellations used in most communication systems, such as high-order QAM constellations, do not have the uniform error property [18]. Therefore, to determine the distance spectrum of a NB convolutional code associated with a high order modulation, we have to consider all possible pairs of competing sequences, with paths diverging from a given state in the trellis diagram and then converging again to a given state. Such sequence pairs are called DC (diverging and converging) sequences or paths within this paper. The corresponding cumulated Euclidean distance is computed as the sum of the Euclidean distances between symbols transmitted along the two DC paths.

For DC paths stretching over L trellis sections, the squared cumulated Euclidean distance between two DC sequences X^1 and X^2 is calculated as follows:

$$\begin{aligned} D^2_{Euc} &= \sum_{l=1}^{L} \left(d^2(X^1_{ls}, X^2_{ls}) + d^2(X^1_{lp}, X^2_{lp}) \right) \\ &= \sum_{l=1}^{L} \Big[(I_{X^1_{ls}} - I_{X^2_{ls}})^2 + (Q_{X^1_{ls}} - Q_{X^2_{ls}})^2 \\ &\quad + (I_{X^1_{lp}} - I_{X^2_{lp}})^2 + (Q_{X^1_{lp}} - Q_{X^2_{lp}})^2 \Big] \end{aligned} \tag{10}$$

where X^b_{ls} and X^b_{lp} are the systematic and parity values respectively, at trellis section l in sequence X^b, $b = 1, 2$, and I_x and Q_x represent the in-phase and quadrature components of constellation signal x.

The search for good NB convolutional codes consists in searching for the set of coefficients α_1, α_2 and α_3 that maximize the lowest D_{Euc} values while minimizing their multiplicities (i.e. the number of sequence pairs with a given distance).

B. Distance spectrum computation methodology

The distance spectrum of a NB code can be calculated by enumerating the DC sequences in the code trellis and by computing the corresponding cumulated Euclidean distances according to (10). For the NB code model adopted in our study (structure S_2 in Fig. 2), the trellis is fully connected. Therefore, any pair of paths in the trellis diverging from a state at time i can converge to any state at time $i+2$, i.e., the shortest DC sequences have length 2. We have observed that, whatever the values of coefficients α_1, α_2 and α_3, enumerating the length-2 and length-3 DC pairs of paths (see Fig. 3) is enough to find all the sequences corresponding to the minimum cumulated Euclidean distance d_1 and to the second minimum cumulated Euclidean distance d_2 of the code. This is guaranteed since, when considering length-3 sequences diverging from a state but not converging to another (see truncated DC-4 sequences in Fig. 3), the obtained cumulated distances are greater than d_1 and d_2.

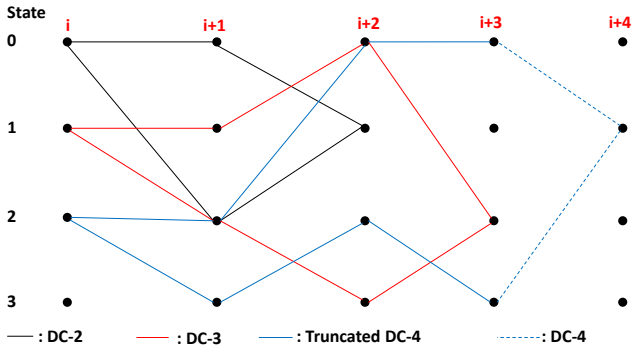


Fig. 3. Examples of length-2, length-3, truncated length-4 and length-4 DC pairs of sequences in GF(4).

Therefore, for each examined code, we have enumerated length-2 and 3 DC sequences, computed the corresponding

cumulated Euclidean distances and stored the multiplicities for the two first distance terms d_1 and d_2.

C. Search for convolutional codes over GF(q), $q > 2$, with conventional q-QAM constellations

As described in section II, the code is defined through the choice of the coefficients α_1, α_2 and α_3. The selection of the coefficient values defining the best code depends on the mapping of the encoded symbols X in GF(q) to the q-ary constellation $\mathcal{C}$. A question that arises is whether changing the mapping has an impact on the distance spectrum of the best convolutional code that can be found by varying the coefficients α_1, α_2 and α_3. For a q-ary constellation $\mathcal{C}$, $q!$ different mappings μ can be defined. Since the values of the first and second minimum cumulated Euclidean distances, and their multiplicities, are calculated from length-2 and 3 DC sequences as stated in section III-B, the study of the effect of changing the mapping μ on these sequences should be performed to answer this question. Two cases are considered for this study:

- The code is defined and kept unchanged (constant values are taken for the α_j parameters, $j = 1 \cdots 3$), while the constellation mapping μ spans the different $q!$ possibilities,
- The mapping μ is kept unchanged, while each α_j code parameter spans the $q-1$ possible values.

If both cases provide two coded modulations with the same distance spectrum, we can then conclude that the mapping has no impact on the result of the search procedure.

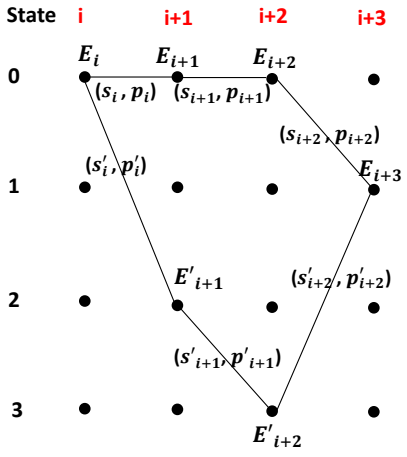


Fig. 4. An example of length-3 DC sequences in a GF(4) code trellis.

Fig. 4 shows an example of two DC sequences of length-3. The exploration of such DC sequences can be divided into three steps:

- The first step focuses on the divergence section of the sequences, i.e. the section where they first diverge from the same state E_i to two different states E_{i+1} and E'_{i+1}.
- The second step addresses the trellis section (or sections for longer sequences) where these sequences do not have any state in common. This step corresponds to the transitions from E_{i+1} to E_{i+2} and from E'_{i+1} to E'_{i+2} in the example of Fig. 4. Note that for length-2 DC sequences, this step does not exist.
- The final step concerns the trellis section where the sequences converge to the same state E_{i+3}.

The exploration consists of counting the total number of different possible cumulated Euclidean distances between DC sequences for each of the two previously mentioned study cases. It is performed for the general assumption of an arbitrarily shaped q-ary constellation, which represents the worst case scenario. For QAM constellations, symmetry could be exploited to reduce the number of different possible Euclidean distances.

a) Case 1 – α_j parameters are constant and μ changes: Let N_μ denote the number of different possible values of the cumulated Euclidean distance between any two DC sequences of length up to 3, when μ changes.

- Step 1: The Euclidean distances are computed between transitions labeled by systematic and parity symbols emanating from the same state. They are divided into two sub-terms, one for the systematic part and one for the parity part (see (10)). The number of differently valued sub-terms for each symbol type is the number of combinations of 2 in a set of q elements, denoted by $\binom{q}{2}$. When varying the mapping, any combination of any two possible values of each symbol type is possible. Therefore, the contribution of step 1 to N_μ is $\binom{q}{2}^2$.
- Step 2: The Euclidean distances are computed between transitions without any state in common. Contrary to step 1, the transitions with equal values of systematic ($s_{i+1} = s'_{i+1}$) or parity ($p_{i+1} = p'_{i+1}$) symbols should also be considered. Therefore, the contribution of step 2 to N_μ is $\left(\binom{q}{2}+1\right)^2 - 1$. The omitted term corresponds to the non-existing case where ($s_{i+1} = s'_{i+1}$) and ($p_{i+1} = p'_{i+1}$), due to the code structure, following (5) and (7).
- Step 3: Dictated by the code structure, by exploiting the existing symmetry with regards to step 1, we can deduce that the contribution of step 3 to N_μ is also $\binom{q}{2}^2$.

In summary, $N_\mu = \left(\left(\binom{q}{2}+1\right)^2 - 1\right) \cdot \binom{q}{2}^4$.

b) Case 2 – μ is constant and α_j parameters change: Let N_α denote the number of different possible values of the cumulated Euclidean distance between any two DC sequences of length up to 3, when varying α_j values.

- Step 1: When emanating from the same state, the transitions are labeled by all the possible systematic symbols. This corresponds to $\binom{q}{2}$ different possible sub-terms in the Euclidean distance. When varying the α_j parameters, if all combinations of q^2 parities labeling any couple of transitions are spanned, then the ensemble of generated codes covers all possible parity symbol combinations. This can be verified by taking one reference transition (systematic and parity values kept constant) and by validating that the second transition can span all possible parity values, even when the systematic part is constant.

In Fig. 4, for the same starting state E_i, if transition (s_i, p_i) is taken as a reference, then parity p'_i should be able to span the $q-1$ possible values (excluding $p_i = p'_i$) when s'_i is kept unchanged. From (5) and (7), we have:

$$p_i + p'_i = \alpha_2(s_i + s'_i) \tag{11}$$

When α_2 spans GF(q), $p_i + p'_i$ takes the $q-1$ different non zero values. Therefore, p'_i can actually take any possible value in $\{\text{GF}(q)\backslash\{p_i\}\}$. Consequently, the contribution of step 1 to N_α is $\binom{q}{2}^2$.

- Step 2: With code structure S_2, q^2 different competing transitions are considered in this step regardless of the code parameters α_j, since any two transitions differ at least by their systematic or parity value. Therefore, the contribution of step 2 to N_α is $\binom{q^2}{2}$.
- Step 3: Again, dictated by the code structure, by exploiting the existing symmetry with regards to step 1, the contribution of step 3 to N_α is $\binom{q}{2}^2$.

In summary, $N_\alpha = \binom{q^2}{2} \cdot \binom{q}{2}^4$.

The comparison of N_μ with N_α allows us to determine if the mapping plays a role in the definition of the best code distance spectrum. $\binom{q}{2}^4$ is a common factor of N_μ and N_α, it is then sufficient to compare the terms $\binom{q^2}{2}$ and $\left(\binom{q}{2}+1\right)^2 - 1$:

$$\begin{aligned} \delta_N &= \binom{q^2}{2} - \left(\binom{q}{2}+1\right)^2 + 1 \\ &= \frac{q^2(q^2-1)}{2} - \frac{q(q-1)(q^2-q+4)}{4} \\ &= \frac{q(q-1)^2(q+4)}{4} > 0 \;\forall\; q > 0 \end{aligned} \tag{12}$$

Since $\delta_N > 0$, then $N_\alpha > N_\mu$. In conclusion, varying the code parameters α_j is sufficient to find the best code using the proposed search procedure. Therefore, in the rest of the paper, the mapping function μ is kept constant and is given in Table I for 16-QAM and 64-QAM constellations. It was chosen such that the binary image of the constellation symbol follows a Gray mapping. The binary images of the symbols are denoted by $b_3b_2b_1b_0$ and $b_5b_4b_3b_2b_1b_0$ for 16-QAM and 64-QAM, respectively, with the highest index corresponding to the most significant bit of the symbol representation.

Using the NB convolutional code structure S_2 depicted in Fig. 2, the first terms of the distance spectra for all possibles codes in GF(16) and GF(64) were determined by varying coefficients α_1, α_2 and α_3, according to the methodology proposed in Section III-B. The primitive polynomials used to generate the elements of the Galois fields are: $P_{\text{GF(16)}}(D) = 1 + D^3 + D^4$ and $P_{\text{GF(64)}}(D) = 1 + D^2 + D^3 + D^5 + D^6$.

Table II provides the values of coefficients α_1, α_2 and α_3 for three specific codes resulting from the search in GF(16) and in GF(64). In each field, C_1 is a code instance showing the worst distance spectrum, C_3 is a code instance showing the best distance spectrum, and code C_2 is a code with a "medium" distance spectrum. Table II also displays the corresponding distance spectra truncated to the first two minimum distances d_1 and d_2, with their multiplicities $n(d_1)$ and $n(d_2)$, i.e. the number of DC sequences with distances d_1 and d_2.

TABLE I
BINARY MAPPING OF THE IN-PHASE I AND QUADRATURE Q AXES FOR 16- AND 64-QAM.

16-QAM			
Q value	b_3b_1	I value	b_2b_0
+3	00	+3	00
+1	01	+1	01
-1	11	-1	11
-3	10	-3	10
64-QAM			
Q value	$b_5b_3b_1$	I value	$b_4b_2b_0$
+ 7	000	+ 7	000
+5	001	+5	001
+3	011	+3	011
+1	010	+1	010
-1	110	-1	110
-3	111	-3	111
-5	101	-5	101
-7	100	-7	100

TABLE II
THREE REPRESENTATIVE CODES OBTAINED FROM THE SEARCH OVER GF(16) AND GF(64), WITH THE TWO FIRST TERMS OF THE SQUARED EUCLIDEAN DISTANCE SPECTRA d_1^2 AND d_2^2 AND THE CORRESPONDING MULTIPLICITIES $n(d_1)$ AND $n(d_2)$.

GF(16)			
Code	C_1	C_2	C_3
$(\alpha_1, \alpha_2, \alpha_3)$	$(12, 4, 0)$	$(10, 12, 3)$	$(13, 7, 11)$
d_1^2 (d_{min}^2)	1.20	2.00	4.00
$n(d_1)$	22128	5532	22484
d_2^2	1.60	2.40	4.80
$n(d_2)$	16596	8424	141144
GF(64)			
Code	C_1	C_2	C_3
$(\alpha_1, \alpha_2, \alpha_3)$	$(41, 2, 0)$	$(41, 1, 24)$	$(31, 5, 18)$
d_1^2 (d_{min}^2)	0.38	1.14	1.52
$n(d_1)$	238422	1542390	652698
d_2^2	0.57	1.23	1.61
$n(d_2)$	230886	4111444	1084014

IV. SIMULATION RESULTS

The error rate performance of the selected codes was assessed through Monte Carlo simulations over a Gaussian channel. We simulated the transmission of blocks of 100 symbols, corresponding to 400 bits in the case of GF(16) and 600 bits in the case of GF(64), decoded with the well-known Max-Lop-MAP algorithm [21]. The symbol error rate curves are shown in Figure 5 for the codes in GF(16) and in Figure 6 for the codes in GF(64). These figures show the range of performance that can be obtained with the proposed code structure and search process. We have also checked that several code instances with the same distance spectra display the same error rate performance (which is not shown in this paper for the sake of concision).

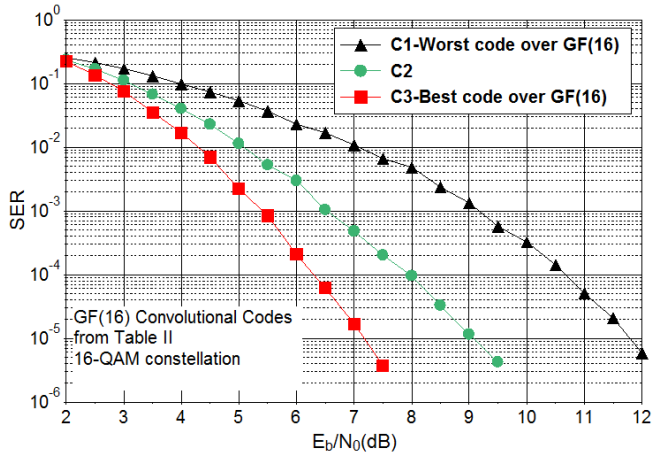


Fig. 5. Performance comparison of convolutional codes over GF(16) in terms of symbol error rates over the AWGN channel.

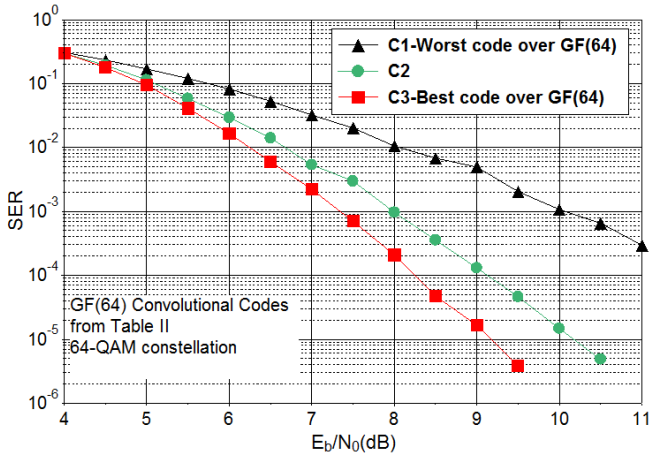


Fig. 6. Performance comparison of convolutional codes over GF(64) in terms of symbol error rates over the AWGN channel.

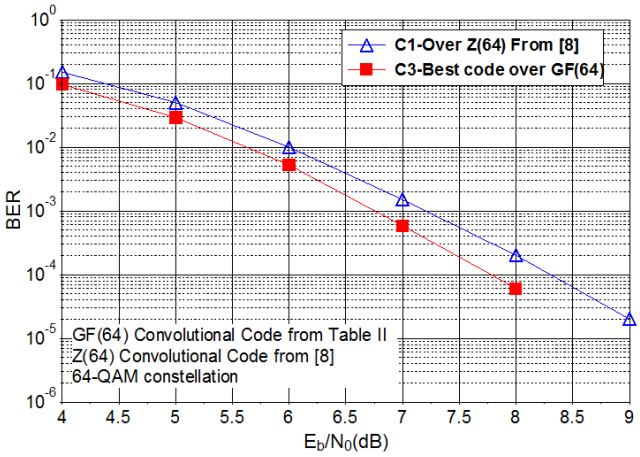


Fig. 7. Performance comparison of the proposed convolutional code defined over GF(64) (code C_3) with the code defined over $\mathbb{Z}_{64}$ and labeled C_1 in [8], in terms of bit error rate. Transmission is over an AWGN channel using 64-QAM constellation.

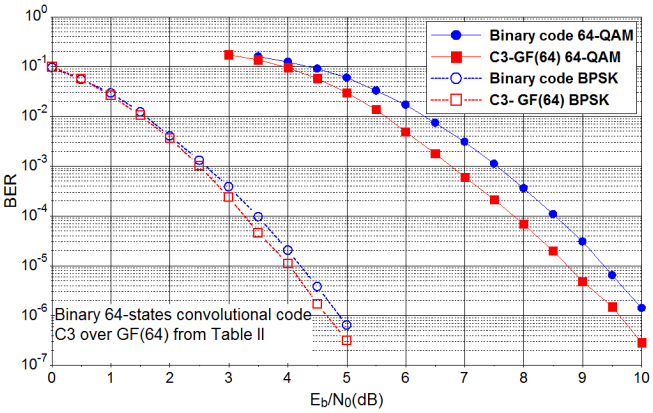


Fig. 8. Performance comparison of the proposed convolutional codes over GF(64) with the best known 64-state-binary code in terms of bit error rate. Transmission is over an AWGN channel, using BPSK and 64-QAM constellations.

In [8], the construction of non-binary convolutional codes over rings was proposed and assessed in the case of AWGN channel. For the code defined over $\mathbb{Z}_{64}$, the resulting coded symbols are directly mapped to a 64-QAM constellation. Fig. 7 shows the comparison in terms of bit error rate of our best code over GF(64) (C_3), with the best code defined in [8] over $\mathbb{Z}_{64}$. This comparison shows that our best code in GF(64) outperforms by around 0.5 dB the best proposed code over $\mathbb{Z}_{64}$.

In addition, the designed NB code over GF(64) was compared with the binary 64-state recursive systematic convolutional code with generator polynomials $\left(1, \frac{171}{133}\right)$ in octal. The latter is known to be the 64-state binary recursive systematic convolutional code with the highest minimum Hamming distance [22]. Bit error rate curves were plotted for both BPSK and 64-QAM constellations. The curves in Fig. 8 show that, when combined with a 64-QAM, the designed NB code yields a gain in the order of 0.7 dB in comparison with the binary code, which is in accordance with the gain predicted by the capacity comparison in Fig. 1 at coding rate $1/2$. In addition, when used with a BPSK modulation, the NB code still shows a slightly better performance than the binary code, although no capacity gain was expected.

V. Conclusion

This paper presents a general framework for the design of recursive systematic convolutional codes defined over high-order Galois fields. A new low-complexity structure of convolutional codes is proposed, using only one memory element. This structure allows the search space for the code to span all the combinations of systematic and parity symbols for each transition between two states in the trellis. It was also shown that the distance properties of the resulting codes are independent of the constellation mapping. The designed codes offer better performance than the non-binary codes previously proposed in the literature. They also outperform their binary counterparts when combined with their corresponding QAM

modulation or with lower order modulations. This study can be considered as a first step to design non-binary turbo codes. The exploration of interleaving techniques, puncturing patterns and the reduction of the decoding complexity can be identified as the next steps to complete this work.

ACKNOWLEDGMENT

This work was partially funded by the EPIC project of the European Union's Horizon 2020 research and innovation programme under grant agreement No. 760150.

REFERENCES

[1] C. Berrou, A. Glavieux, and P. Thitimajshima, "Near shannon limit error-correcting coding and decoding: Turbo-codes," in *IEEE Int. Conf. Communications, (ICC'93)*, vol. 2, Geneva, Switzerland, May 1993, pp. 1064–1070.

[2] R. Gallager, "Low-density parity-check codes," *IRE Trans. Inform. Theory*, vol. 8, no. 1, pp. 21–28, 1962.

[3] D. J. MacKay and R. M. Neal, "Near shannon limit performance of low density parity check codes," *Electron. Lett.*, vol. 32, no. 18, pp. 1645–1646, Aug. 1996.

[4] G. Liva, L. Gaudio, T. Ninacs, and T. Jerkovits, "Code design for short blocks: A survey," *arXiv preprint arXiv:1610.00873*, 2016.

[5] J. Hokfelt, O. Edfors, and T. Maseng, "Turbo codes: Correlated extrinsic information and its impact on iterative decoding performance," in *IEEE 49th Vehicular Technology Conf.*, vol. 3, Houston, TX, USA, 1999, pp. 1871–1875.

[6] M. C. Davey and D. J. MacKay, "Low density parity check codes over GF(q)," *IEEE Commun. Lett.*, vol. 2, no. 6, pp. 165–167, June 1998.

[7] C. Poulliat, M. Fossorier, and D. Declercq, "Design of regular (2, dc)-LDPC codes over GF(q) using their binary images," *IEEE Trans. Commun.*, vol. 56, no. 10, pp. 1626–1635, Oct. 2008.

[8] T. Konishi, "A coded modulation scheme for 64-QAM with a matched mapping," in *IEEE Int. Symp. Inform. Theory and its Applications (ISITA)*, Oct. 2014, pp. 191–195.

[20] D. Divsalar and M. Simon, "Trellis coded modulation for 4800-9600 bits/s transmission over a fading mobile satellite channel," *IEEE J. Select. Areas in Commun.*, vol. 5, no. 2, pp. 162–175, Feb. 1987.

[9] G. Liva, S. Scalise, E. Paolini, and M. Chiani, "Turbo codes based on time-variant memory-1 convolutional codes over Fq," in *IEEE Int. Conf. Communications*, Kyoto, Japan, June 2011, pp. 1–6.

[10] G. Liva, E. Paolini, B. Matuz, S. Scalise, and M. Chiani, "Short turbo codes over high order fields," *IEEE Trans. Commun.*, vol. 61, no. 6, pp. 2201–2211, June 2013.

[11] Y. Zhao, "Convolutional codes defined in GF(q) combine with PNC over impulsive noise channels," in *IEEE Int. Conf. for Students on Applied Engineering (ICSAE)*, Newcastle upon Tyne, UK, Oct. 2016, pp. 142–146.

[12] Y. Zhao, M. Johnston, C. Tsimenidis, and L. Chen, "Non-binary turbo-coded physical-layer network coding on impulsive noise channels," *Electron. Lett.*, vol. 52, no. 24, pp. 1984–1986, 2016.

[13] W. Abd-Alaziz, M. Johnston, and S. Le Goff, "Non-binary turbo codes on additive impulsive noise channels," in *the 10th Int. Symp. Commun. Systems, Networks and Digital Signal Process. (CSNDSP)*, Prague, Czech Republic, July 2016, pp. 1–5.

[14] W. Abd-Alaziz, Z. Mei, M. Johnston, and S. Le Goff, "Non-binary turbo-coded OFDM-PLC system in the presence of impulsive noise," in *the 25th Eur. Signal Process. Conf. (EUSIPCO)*, Kos, Greece, 2017, pp. 2576–2580.

[15] A. Alvarado, "On bit-interleaved coded modulation with QAM constellations," 2008.

[16] G. Caire, G. Taricco, and E. Biglieri, "Bit-interleaved coded modulation," *IEEE Trans. Inform. Theory*, vol. 44, no. 3, pp. 927–946, 1998.

[17] G. Ungerboeck, "Channel coding with multilevel/phase signals," *IEEE Trans. Inform. Theory*, vol. 28, no. 1, pp. 55–67, 1982.

[18] S. Benedetto and E. Biglieri, *Principles of digital transmission: with wireless applications*. Springer Science & Business Media, 1999.

[19] M. K. Simon, B. Levitt, J. Omura, and R. Scholtz, "Spread spectrum communications. volume 1, 2 & 3," *NASA STI/Recon Technical Report A*, vol. 87, 1985.

[21] L. Bahl, J. Cocke, F. Jelinek, and J. Raviv, "Optimal decoding of linear codes for minimizing symbol error rate (corresp.)," *IEEE Trans. Inform. Theory*, vol. 20, no. 2, pp. 284–287, 1974.

[22] P. Frenger, P. Orten, and T. Ottosson, "Convolutional codes with optimum distance spectrum," *IEEE Commun. Lett.*, vol. 3, no. 11, pp. 317–319, 1999.